

Attenuation of hind-limb suspension-induced bone loss by curcumin is associated with reduced oxidative stress and increased vitamin D receptor expression

M. Xin¹ · Y. Yang¹ · D. Zhang² · J. Wang³ · S. Chen⁴ · D. Zhou¹

Received: 9 December 2014 / Accepted: 26 April 2015 / Published online: 12 May 2015
© International Osteoporosis Foundation and National Osteoporosis Foundation 2015

Abstract

Summary Treatment with curcumin attenuated modeled microgravity-induced bone loss, possibly through abating oxidative stress and activating vitamin D receptor. Curcumin might be an effective countermeasure for microgravity-induced bone loss but remains to be tested in humans.

Introduction Bone loss is one of the most important complications for human crewmembers who are exposed to long-term microgravity in space and also for bedridden people. The aim of the current study was to elucidate whether treatment with curcumin attenuated bone loss induced by microgravity.

Methods We used hind-limb suspension (HLS) and rotary wall vessel bioreactor (RWVB) to model microgravity in vivo and in vitro, respectively. We investigated the effects of curcumin consumption (40 mg kg⁻¹ body weight day⁻¹, via daily oral gavages) on Sprague–Dawley (SD) rats exposed to HLS for 6 weeks. Then, we investigated the effects of

incubation with curcumin (4 μM) on MC3T3-E1 and RAW264.7 cells cultured in RWVB.

Results Curcumin alleviated HLS-induced reduction of bone mineral density in tibiae and preserved bone structure in tibiae and mechanical strength in femurs. Curcumin alleviated HLS-induced oxidative stress marked by reduced malondialdehyde content and increased total sulfhydryl content in femurs. In cultured MC3T3-E1 cells, curcumin inhibited modeled microgravity-induced reactive oxygen species (ROS) formation and enhanced osteoblastic differentiation. In cultured RAW264.7 cells, curcumin reduced modeled microgravity-induced ROS formation and attenuated osteoclastogenesis. In addition, curcumin upregulated vitamin D receptor (VDR) expression in femurs of rats exposed to HLS and MC3T3-E1 cells exposed to modeled microgravity.

Conclusion Curcumin alleviated HLS-induced bone loss in rats, possibly via suppressing oxidative stress and upregulating VDR expression.

Keywords Microgravity · Orally · Rats · Reactive oxygen species · Rotary wall vessel bioreactor

Electronic supplementary material The online version of this article (doi:10.1007/s00198-015-3153-7) contains supplementary material, which is available to authorized users.

✉ D. Zhou
zhouds2014@hotmail.com

¹ Department of Orthopaedics, Provincial Hospital Affiliated to Shandong University, 324 JingWu Road, 250021 Jinan, China

² Department of Anaesthesiology, The Second Hospital Affiliated to Shandong University, 250033 Jinan, China

³ The Medical School, The Australian National University, Acton, ACT 0200, Australia

⁴ Research School of Physics and Engineering, The Australian National University, Acton, ACT 0200, Australia

Introduction

The microgravity environment experienced by human crewmembers during space flight or patients during long-term bed rest has an immediate impact on many of the body's biological systems. One of the most significant effects as a result of exposure to microgravity is bone loss, which leads to an increase in fracture risk [1]. Long-term exposure to a microgravity environment leads to enhanced bone resorption in the early phase and then a sustained reduction in bone formation for the duration of weightlessness [2]. Knowledge of microgravity-induced bone loss and the development of

anti-catabolic strategies that retard bone loss are important and challenging for the care of the geriatric population and astronauts.

Curcumin (1,7-bis(4-hydroxy-3-methoxyphenyl)-1,6-heptadiene-3,5-dione) is a phenolic natural product isolated from the rhizome of *Curcuma longa* (turmeric). It has been widely used in Eastern populations, particularly as a traditional medicine in India and China, for the treatment of many diseases, including diabetes and diseases of the hepato-biliary, skin, rheumatoid, and gastrointestinal system [3, 4]. Recently, curcumin has caught scientific attention as a potential therapeutic agent in ovariectomized mature rodent model of postmenopausal osteoporosis [5, 6] and experimental periodontitis bone loss model [7]. In addition, treatment with curcumin improved bone microarchitecture and enhanced mineral density in APP/PS1 transgenic mice, a model of Alzheimer's disease [8]. Furthermore, it has been reported that curcumin is a bifunctional antioxidant [9] because of its ability to react directly with reactive species and to induce an upregulation of various cytoprotective and antioxidant proteins. In addition, curcumin is able to bind vitamin D receptor (VDR), induce recruitment of its co-receptor retinoid X receptor, co-activator steroid receptor co-activator-1, and activate transcription of a VDR-target gene [10].

In the present study, we explored whether long-term treatment with curcumin had beneficial effect in rats exposed to hind-limb suspension (HLS) *in vivo* and its underlying mechanism. In addition, we explored the effect of incubation with curcumin on osteoblastic and osteoclastic function in MC3T3-E1 cells and RAW264.7 cells cultured in rotary wall vessel bioreactor.

Materials and methods

Animals

Sprague–Dawley (SD; male, 8 weeks old) rats were purchased from the Vital-Aiver Animal Ltd (Beijing, China). All the rats were fed under controlled temperature (23 ± 2 °C), 12-h light and 12-h dark cycles (light, 08:00–20:00 hours; darkness, 20:00–08:00 hours) and had free access to food and tap water. All the animals used in this work received humane care in compliance with institutional animal care guidelines. All the surgical and experimental procedures were in accordance with institutional animal care guidelines and were approved by the Local Institutional Committee. Chemicals, drugs, and reagents were obtained from Sigma Chemical (St. Louis, MO, USA) unless otherwise stated. Cell culture supplies were obtained from Invitrogen except where indicated.

SD rats were divided into 4 groups of 12 animals each and treated for 6 weeks as follows: (1) control rats treated with vehicle (Con); (2) HLS rats treated with vehicle; (3) control

rats treated with curcumin (Con+CUR); (4) hind-limb-suspended rats treated with curcumin (HLS+CUR). Six weeks later, the extent of bone loss and oxidative stress-related markers were measured. Palm oil (Merck, Germany) was used as vehicle. The 40-mg/kg dose of curcumin was freshly prepared in 1.0 ml of palm oil [6]. The treatments were given via daily oral gavages for 6 weeks. The dose of curcumin was chosen according to previous positive results in ovariectomized rats. The 110-mg/kg dose of curcumin was used in rats orally, and no significant side effect was reported [6]. In addition, oral administration is convenient for long-term treatment. Daily food consumption was estimated twice 1 week before the experiment and controlled during the treatment.

Cell culture

MC3T3-E1 cells were placed in osteogenic media (DMEM with 10 % FBS, 1 % penicillin-streptomycin, 10 mmol/l β -glycerophosphate, and 50 μ g/ml ascorbic acid) to induce cell differentiation.

The MC3T3-E1 cells were exposed to modeled microgravity and treated with curcumin (4 μ M) for 96 h. The intracellular reactive oxygen species (ROS), osteoprotegerin (OPG), and receptor activator of NF κ B ligand (RANKL) content in supernatant and the messenger RNA (mRNA) levels of VDR were determined.

The MC3T3-E1 cells were exposed to modeled microgravity and treated with curcumin (4 μ M) or 1,25-dihydroxyvitamin D (1,25D; 10 nM) or curcumin+1,25D. The intracellular ROS, OPG, and RANKL content in supernatant were determined.

The RAW264.7 cells were exposed to modeled microgravity and treated with curcumin (4 μ M) for 96 h. RANKL was used to stimulate osteoclastogenesis. ROS formation, CathK and TRAP mRNA expression, and osteoclastogenesis were determined.

Hind-limb suspension

Briefly, an orthopedic adhesive tape was applied along the proximal one third of the tail and placed through a metal ring, which attached to a metal bar on the top of a hind-limb suspension cage. This allowed the forelimbs to have contact with the grid bottom of the cage such that the animals could move and access food and water freely. The suspension height was adjusted to maintain a suspension angle of 30° and to ensure that the hind-limbs were unable to touch any supporting surface. The animals were suspended for a total of 6 weeks. During the tail-suspension period, rats were carefully monitored several times a day to prevent restriction of tail growth and circulation and ensure adequate food and water intake, grooming behavior, urination, and defecation. Control rats

were housed individually in the same size cage as HLS rats. They have tail harnesses on but not suspended. They were allowed to move unconstrained around the cages. All animals of HLS group completed the full 6 weeks.

In vitro-simulated microgravity

The rotary wall vessel bioreactor (RWVB; Synthecon, Houston, TX, USA) was used to model microgravity in vitro according to the method previously described [11]. Briefly, cultured cells (1×10^6 /ml) transferred to the bioreactor and incubated in a 37 °C, 5 % CO₂ incubator without rotation for 1 h to allow cells to attach to the microcarrier beads (Cytodex-3 porous collagen-I-coated microcarrier beads, Sigma). Then, they were rotated about a horizontal axis perpendicular to the gravitational vector to randomize gravitational vectors across the surface of the platelets and generate microgravity of 10^{-2} G. Cells were rotated about a vertical axis parallel to the gravitational vector to experience normal gravitational forces (1 G) and serve as control.

Sample preparation and biochemical analysis

At the end of the experimental period, all rats were fasted for 12 h and anesthetized with ketamine (150 mg/kg)/xylazine (18 mg/kg) mixture, after which whole blood sample was collected from their abdominal aorta. The blood samples were centrifuged at $4000 \times g$ for 10 min, and serum was collected and stored at -20 °C until use. 1, 25-(OH)₂D₃ levels were measured from serum by enzyme immunoassay according to the manufacturer's protocol (ImmunoDiagnostic Systems Ltd, Boldon, UK).

Measurement of deoxyypyridinoline

Urinary deoxyypyridinoline (DPD; the breakdown product of collagen during bone resorption) is a bone resorption marker. DPD excretion was quantified by using an EIA kit (Wuhan Xinqidi Biological Technology, Hubei, China), and the data were corrected for the urinary creatinine levels. Creatinine (CRE) levels were determined with QuantiChrom Creatinine Assay Kits (Shanghai Westtang Bio-Tech, Shanghai, China).

Bone homogenates and measurement of malondialdehyde levels

After the rats were killed, the femurs were excised from each rat and cleaned soft tissue, including cartilage, tendon, and ligament. The femurs were stored in liquid nitrogen at first and then stored at -80 °C until use. The frozen distal femurs were put in a mortar and pestle which contained liquid nitrogen and ground to a fine powder immersed in liquid nitrogen. The frozen powder was transferred into a tube containing $1 \times$

RIPA buffer (50 mM Tris-HCl, pH=8, with 150 mM NaCl, 1.0 % NP-40, 0.5 % sodium deoxycholate, 0.1 % SDS; Beyotime, Jiangsu, China) supplemented with 1 mM phenylmethylsulphonyl fluoride and protease inhibitor cocktail. The protein concentration was determined with bovine serum albumin as a standard by a Bradford assay.

Malondialdehyde (MDA) is a presumptive marker of oxidant-mediated lipid peroxidation. Bone homogenates and plasma were used for the determination of MDA by using a kit (Cayman, Ann Arbor, MI, USA). MDA levels of bone homogenates were normalized to their protein concentration.

Western blotting analysis

Proteins (30 µg/lane) were separated by SDS-PAGE (10 % gel). The gels were electroblotted onto polyvinylidene fluoride membranes (Hybond-P, Amersham International, Little Chalfont, Buckinghamshire, UK) for 1 h at 100 V. The efficiency of the transfer was evaluated using Ponceau red staining according to the manufacturer's conditions. The membranes were incubated with primary antibodies against VDR (Santa Cruz, CA, USA). After washing, the membranes were incubated with HRP-conjugated secondary antibody. After thorough washing, immunocomplexes were detected using an enhanced horseradish peroxidase/luminal chemiluminescence system (ECL Plus, Amersham International, Little Chalfont, UK). Signals on the immunoblot were quantified with the NIH Image V1.56 computer program. Each membrane was reprobbed to determine GAPDH expression using a mouse monoclonal antibody (1:8000, Abcam Cambridge, MA, USA).

Measurement of total sulfhydryl levels

Bone homogenates was used for the determination of total sulfhydryl (t-SH) with Glutathione Assay Kits (Cayman, Ann Arbor, MI, USA). t-SH levels of bone homogenates were normalized to their protein concentration.

Bone mineral density measurement

Bone mineral density (BMD) were measured ex vivo with a dual-energy X-ray absorptiometry NORLAND XR-46 (Norland Co. Fort Atkinson, WI, USA) using the small-animal program set to a high-resolution mode. Samples were placed on an acrylic platform of uniform 38.1-mm thickness. The BMD of whole tibiae was obtained. The coefficient of variation (CV) was 1 % for BMD.

Bone histomorphometry

The proximal tibiae were incubated with the Villanueva bone stain for 7 days, dehydrated in graded ethanol and xylene, and

embedded undecalcified in methyl methacrylate. Frontal sections (4 μm thick) were cut with vertical bed microtomes (Leica, Rockleigh, NJ, USA) and affixed to slides precoated with a 1 % gelatin solution. Then they were stained according to the Von Kossa method with a tetrachrome counterstain (Polysciences, Warrington, PA, USA). Measurements were performed at the metaphyseal region, which was located 1–4 mm from the lowest point of the growth plate and 1 mm from the lateral cortex, excluding the endocortical region. The selected region is known as the secondary spongiosa area, which is rich in trabecular bone. The selected region is squared, and the area of the squared region is about 9 mm² (3×3 mm). Histomorphometric data were collected with the Bioquant Bone Morphometry System (R&M Biometrics Corp., Nashville, TN, USA). Osteoclast surface and osteoblast surface were obtained. Eight bone sections were analyzed per animal.

Micro-CT

Trabecular bone morphometry within the metaphyseal region of proximal tibiae was quantified using micro-CT (μCT40 , Scanco Medical AG, 10.5 μm voxel size, 55 kVp, 145 μA) with a threshold value of 240 as the method described previously [12]. The proximal tibial metaphysis was scanned in 250 slices (thickness, 13 μm) in the dorsoventral direction. Three-dimensional reconstruction of the bone was performed using the triangulation algorithm. Trabecular morphometry was characterized by measuring trabecular bone volume fraction (BV/TV), trabecular thickness (Tb.Th), trabecular separation (Tb.Sp), and trabecular number (Tb.N).

Measurement of mechanical properties

Using a mechanical strength analyzer (CSS-4420 material testing machine, Changchun Research Institute for Testing Machines Co. Ltd., China), the mechanical strength of the left femur was measured.

For the quasi-static 3-point bending test, the left femur was placed on a special holding device with supports located 12 mm apart. Afterwards, the load was applied to the middle part of the diaphysis, thus a three-point bending test was created. A bending force was applied at a speed of 1 mm/min, until a fracture occurred. From the load–displacement curve, the ultimate compressive load (N), the stiffness (N/mm), and the energy absorption (mJ) were obtained from the femoral diaphysis via keeping record of the load and displacement until the specimen was broken. The ultimate load (N) was defined as the maximum load sustained by the specimen, the stiffness (N/mm) was defined as the slope of the linear portion of

the curve, and the energy to ultimate load (mJ) was determined as the area under the curve to ultimate load.

Quantitative real-time PCR analysis

After the rats were killed, the femurs were excised from each rat and cleaned soft tissue including cartilage, tendon, and ligament. The femurs were stored in liquid nitrogen at first and then stored at $-80\text{ }^{\circ}\text{C}$ until use. The frozen distal femurs were put in an RNase-free mortar and pestle which contained liquid nitrogen and ground to a fine powder immersed in liquid nitrogen. The frozen powder was transferred into a tube containing Trizol (Life Technologies Inc. Gaithersburg, USA), and total RNA was isolated, according to the manufacturer's protocol. The RNA purity and concentration were examined on the wavelength ($A_{256\text{ nm}}/A_{280\text{ nm}}$) more than 1.8; 1 μg of total RNA was treated with DNase I (Invitrogen) in a total volume of 10 and 5 μl (500 ng) of this batch was reverse transcribed with 200 U SuperScript II (Invitrogen) using 500 ng oligo-dT and 250 ng random hexamers. RT-PCR analysis was performed with a QuantiTectTM SYBR[®] Green PCR (Qiagen, Shanghai, China) according to the manufacturer's instructions. The RT-PCR data was based on SYBR green amplification. The sequences of primers are listed in Table 1S (Supplementary data). PCR amplification was performed in 96-well optical reaction plates for 40 cycles, with each cycle at $94\text{ }^{\circ}\text{C}$ for 30 s, $58\text{--}63\text{ }^{\circ}\text{C}$ for 30 s, and $72\text{ }^{\circ}\text{C}$ for 60 s. Each sample was run and analyzed in duplicate. Target mRNA levels were adjusted as the values relative to 18S, which was used as the endogenous control to ensure equal starting amounts of cDNA. The fold-change relative to values of control group were obtained and used to express the experimental change in gene expression. Inter-assay variation was less than 10 % coefficient of variation for all quantitative real-time PCR assays.

Reactive oxygen species production

Before incubation in RWVB and treatment with curcumin, the culture medium was replaced with phenol-red-free DMEM containing 2',7'-dichlorodihydrofluorescein diacetate (10 μM , this probe is widely used to monitor the cellular redox processes) for 30 min. Then, remove the dye working solution; wash with pre-warmed medium, and add pre-warmed medium. The ROS production was measured with a fluorescence reader.

Alkaline phosphatase activity assay

The induction of alkaline phosphatase (ALP) is an unequivocal marker for bone cell differentiation. After incubation in

RWVB and treatment with curcumin or 1,25D for 7 days, the medium was removed and the cell monolayer was gently washed twice with PBS. Cells were then lysed with cell lysis buffer and centrifuged at $12,000\times g$ for 10 min. The supernatant was collected and used for the measurement of ALP activity with an ALP activity assay kit (Cell Biolabs, San Diego, CA, USA). ALP activities were normalized to their protein concentration.

Measurement of OPG and receptor activator of NF κ B ligand

After incubation in RWVB and treatment with curcumin for 96 h, the concentrations of OPG and RANKL proteins in the supernatant of cultured MC3T3-E1 cells were measured using their kits (R&D Systems, San Diego, CA, USA). Finally, the ratio of OPG/RANKL was calculated.

Measurement of osteoclastogenesis

RAW264.7 cells at 2.5×10^5 were cultured in RWVB and stimulated with RANKL (20 ng/ml) and treated with curcumin for 4 days. Then, the cells were tartrate-resistant acid phosphatase (TRAP) stained according to the method described previously [13]. For quantification, multinucleated TRAP-positive cells with different number of nuclei were counted in two different categories: 3 to 30 nuclei and those with greater than 30 nuclei.

Statistical analysis

Our results were expressed as mean \pm SD. The coefficient of variation for all assays except RT-PCR experiment was not more than 1 %. One-way ANOVA with Bonferroni's correction for multiple comparisons were applied, and statistical difference was considered with p values <0.05 . Statistical analysis was performed using SPSS 14.0.0 software (SPSS Inc. Chicago, IL, USA).

Results

Effects of treatment with curcumin on general data in rats exposed to HLS

SD rats were exposed to HLS for 6 weeks and treated with or without curcumin. As shown in Table 2S (Supplementary data), the soleus muscle-to-body mass ratios were significantly lower ($p<0.001$) in rats exposed to HLS, which confirmed the efficacy of simulated microgravity in this set of experiments. HLS led to a significant

reduction in body weight ($p<0.001$) and food intake ($p=0.010$), and curcumin treatment had no significant effect on body weight and food intake.

Effects of treatment with curcumin on bone geometric and microstructural parameters of rats exposed to HLS

When compared with the control rats, BMD of the whole tibia (Fig. 1a, $p=0.011$), Ob.S/BS (Fig. 1b, $p<0.001$), Tb.Th (Fig. 1d, $p=0.002$), Tb.N (Fig. 1f, $p<0.001$), and BV/TV (Fig. 1g, $p<0.001$) of proximal tibiae and ultimate load (Fig. 1h, $p=0.007$), stiffness (Fig. 1i, $p<0.001$), and energy (Fig. 1j, $p=0.004$) of femoral diaphysis were lower, and Tb.Sp (Fig. 1e, $p<0.001$) and Oc.S/BS (Fig. 1c, $p<0.001$) of proximal tibiae were higher in HLS rats.

When compared with HLS rats, BMD of the whole tibia (Fig. 1a, $p=0.032$), Ob.S/BS (Fig. 1b, $p<0.001$), Tb.Th (Fig. 1d, $p=0.013$), Tb.N (Fig. 1f, $p=0.018$), and BV/TV (Fig. 1g, $p=0.008$) of the proximal tibiae and ultimate load (Fig. 1h, $p=0.027$), stiffness (Fig. 1i, $p=0.015$), and energy (Fig. 1j, $p=0.021$) of femoral diaphysis were higher, and Tb.Sp (Fig. 1e, $p<0.001$) and Oc.S/BS (Fig. 1c, $p<0.001$) of the proximal tibiae were lower in HLS rats treated with curcumin.

Treatment of control rats with curcumin had no significant effect on these parameters.

As shown in the Supplementary data (Fig. S1), the beneficial effect of curcumin on bone geometric and microstructural parameters of rats exposed to HLS was in a dose-dependent manner.

Effects of treatment with curcumin on the biomarkers of osteoblastogenesis and osteoclastogenesis in femurs of rats exposed to HLS

Compared with the control rats, mRNA levels of TRAP (Fig. 2a, $p<0.001$) and mRNA ratio of RANKL-to-OPG (Fig. 2c, $p<0.001$) of distal femurs and urinary DPD excretion (Fig. 2d, $p<0.001$) were higher in HLS rats, and mRNA levels of osteocalcin (Fig. 2b, $p<0.001$) of distal femurs was lower in HLS rats.

In HLS+curcumin group, mRNA levels of TRAP ($p<0.001$) and mRNA ratio of RANKL-to-OPG of distal femurs ($p<0.001$) and urinary DPD excretion ($p=0.003$) were lower, and mRNA levels of osteocalcin of distal femurs ($p<0.001$) was higher than that in the HLS group.

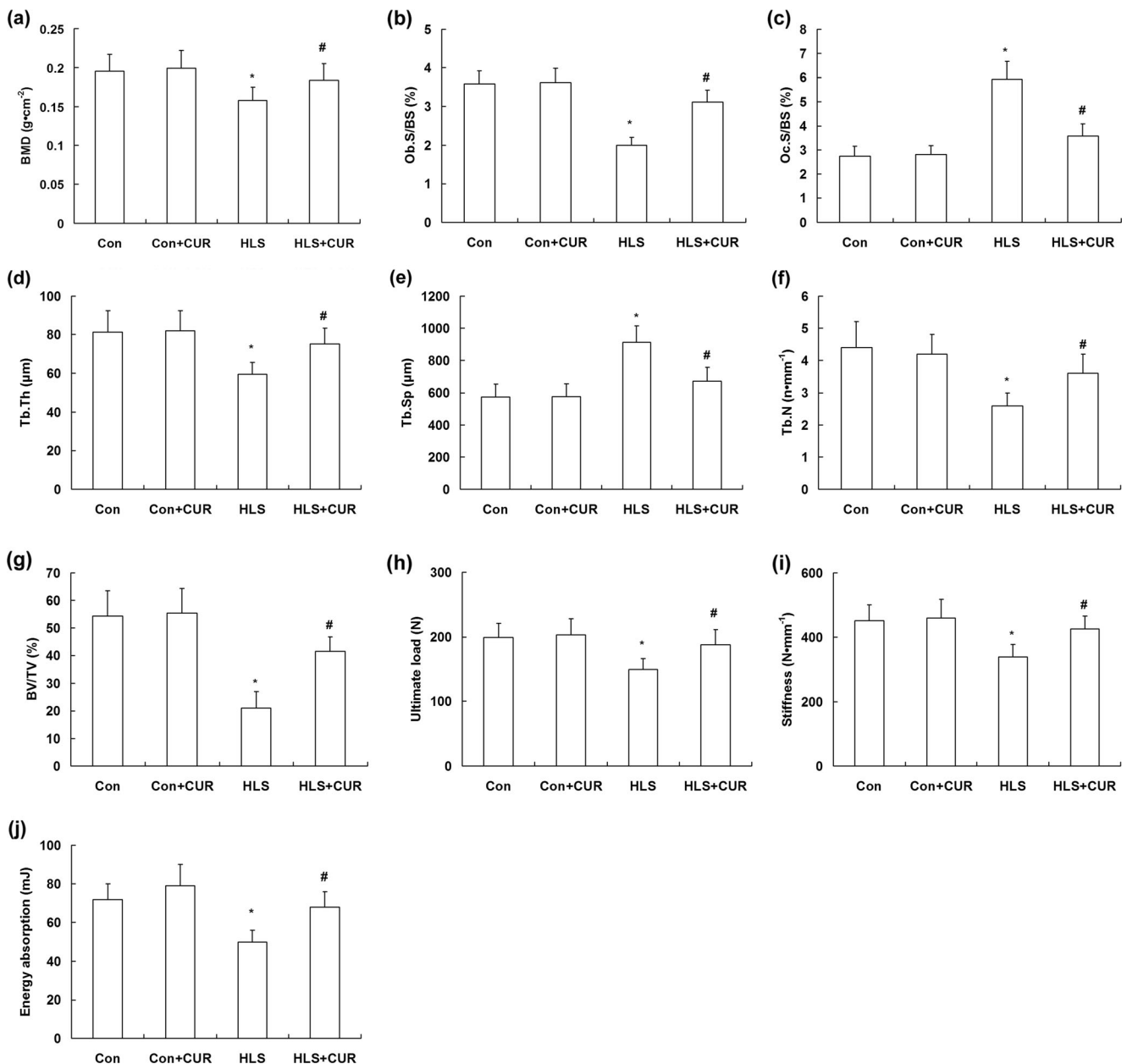


Fig. 1 Curcumin treatment during 6 weeks of HLS mitigates deleterious changes in bone geometry and microarchitecture. SD rats were exposed to HLS and treated with or without curcumin (40 mg/kg body weight) for 6 weeks. Tibiae were removed for the determination of BMD (a), osteoblast (b), and osteoclast (c) surfaces and trabecular morphometry including Tb.Th (d), Tb.Sp (e), Tb.N (f), and bone volume fraction

(BV/TV) (g). Femurs were removed for determination of mechanical properties including ultimate load (h), stiffness (i), and energy (j). $n=12$ in each group. CUR curcumin, HLS hind-limb suspension, BMD bone mineral density, Tb.Th trabecular thickness, Tb.Sp trabecular separation, Tb.N trabecular number; * $p<0.05$ versus control group; # $p<0.05$ versus HLS group

Effect of treatment with curcumin on oxidative stress in femurs of rats exposed to HLS

Compared with the control rats, MDA levels of plasma (Fig. 3a, $p=0.003$) and distal femurs (Fig. 3b, $p=0.006$) were higher, and t-SH levels (Fig. 3c, $p=0.002$) of distal femurs were lower in the HLS group. Treatment with curcumin reduced the levels of MDA in plasma ($p=$

0.011) and distal femurs ($p=0.017$) and enhanced the levels of t-SH in distal femurs ($p<0.001$).

Effects of incubation with curcumin on osteoblast cell line-MC3T3-E1 cultured in RWVB

MC3T3-E1 cells cultured in RWVB showed increased ROS formation (Fig. 4a, $p=0.002$) and reduced osteoblastic

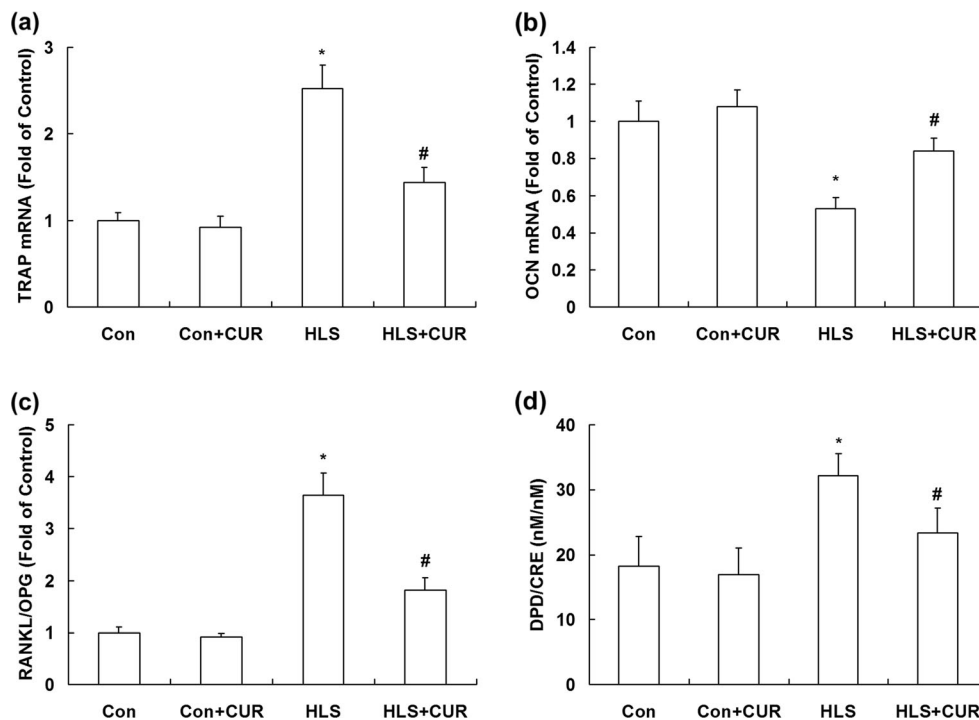


Fig. 2 Curcumin treatment during 6 weeks of HLS enhances osteoblastogenesis and suppresses osteoclastogenesis. SD rats were exposed to HLS and treated with or without curcumin (40 mg/kg body weight) for 6 weeks. Femurs were removed for the determination of mRNA levels of TRAP (a) and OCN (b) and mRNA ratio of RANKL/OPG (c). Urine was collected for determination of DPD excretion

(biomarker of bone resorption, d). $n=12$ in each group. *CUR* curcumin, *HLS* hind-limb suspension, *OCN* osteocalcin, *RANKL* receptor activator of NF- κ B ligand, *OPG* osteoprotegerin, *CRE* creatinine, *TRAP* tartrate-resistant acid phosphatase, *CRE* creatinine, *DPD* deoxypyridinoline; * $p<0.05$ versus control group; # $p<0.05$ versus the HLS group

differentiation marked by decreased ALP activity (Fig. 4b, $p=0.005$). Incubation with curcumin suppressed ROS formation ($p=0.014$) and enhanced osteoblastic differentiation ($p=0.020$).

Exposure to modeled microgravity of MC3T3-E1 cells led to an augmentation of ratio of RANKL/OPG (Fig. 4c, $p<0.001$), which was decreased by treatment with curcumin ($p<0.001$).

Effects of incubation with curcumin on preosteoclast cell line-RAW264.7 cultured in RWVB

RAW264.7 cells cultured in RWVB showed increased ROS formation (Fig. 5a, $p<0.001$) and enhanced osteoclastic differentiation marked by increased CathK (Fig. 5b, $p<0.001$) mRNA levels, and increased osteoclastogenesis marked by increased TRAP mRNA levels (Fig. 5c, $p<0.001$) and TRAP-positive multinucleated osteoclasts (Fig. 5d, $3<\text{nuclei}\leq 30$, $p<0.001$; $\text{nuclei}>30$, $p<0.001$).

Treatment with curcumin reduced ROS levels and suppressed osteoclastic differentiation and osteoclastogenesis marked by reduced mRNA levels of CathK ($p<0.001$) and TRAP ($p<0.001$) and TRAP-positive multinucleated osteoclasts ($3<\text{nuclei}\leq 30$, $p=0.001$; $\text{nuclei}>30$, $p<0.001$).

Effects of treatment with curcumin on VDR expression

Exposure to HLS led to reduction in both serum levels of $1,25\text{-(OH)}_2\text{D}_3$ (Fig. 6a, $p<0.001$) and mRNA levels (Fig. 6b, $p<0.001$) and protein expression (Fig. 6d) of VDR in femurs. Treatment with curcumin did not affect serum levels of $1,25\text{-(OH)}_2\text{D}_3$, but enhanced VDR mRNA levels ($p<0.001$) and upregulated VDR protein expression ($p<0.001$) in rats exposed to HLS.

MC3T3-E1 cells cultured in RWVB showed reduced mRNA levels (Fig. 6c, $p<0.001$) and protein expression (Fig. 6d) of VDR. Treatment with curcumin enhanced VDR mRNA levels ($p<0.001$) and upregulated VDR protein expression ($p<0.001$) in MC3T3-E1 cells cultured in RWVB.

As shown in the Supplementary data (Fig. S2), treatment with 1,25D had no significant effect on ROS formation but suppressed ROS formation and enhanced osteoblastic differentiation marked by increased ALP activity ($p=0.028$) and ratio of RANKL/OPG ($p<0.001$).

Discussion

Microgravity exposure to animals or humans led to oxidative stress not only in circulating system [14]. Sun et al. reported that

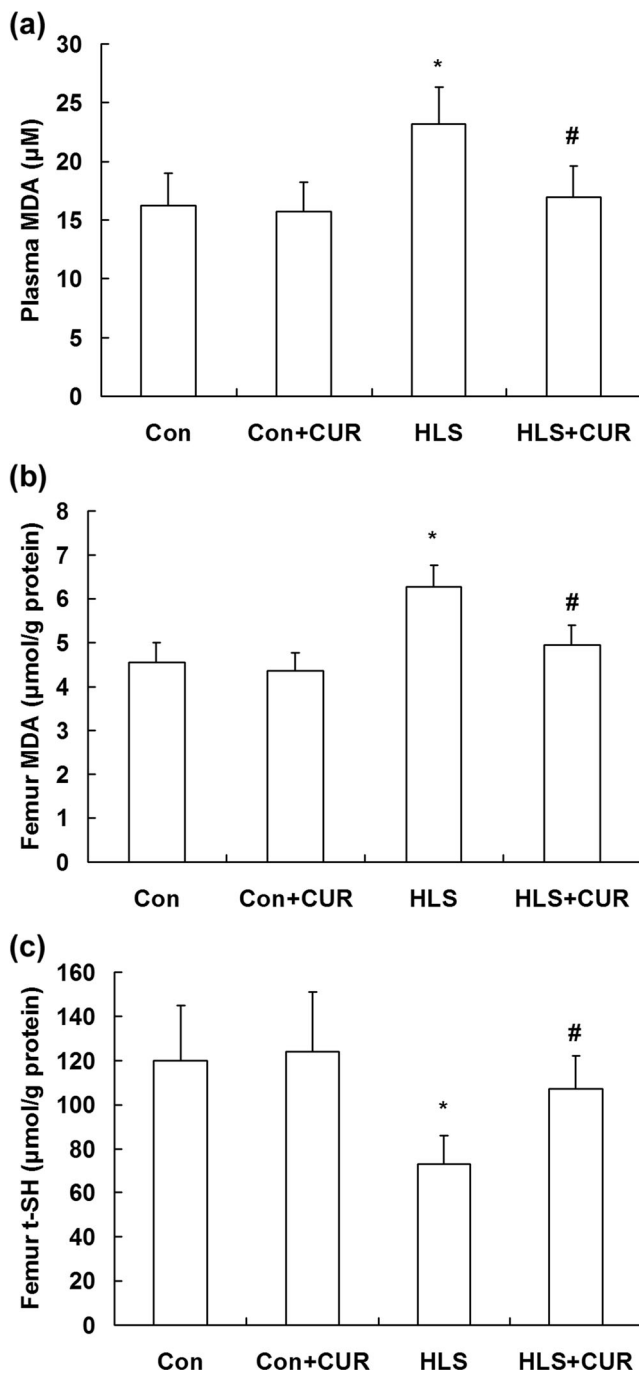


Fig. 3 Curcumin treatment during 6 weeks of HLS abates oxidative stress. SD rats were exposed to HLS and treated with or without curcumin (40 mg/kg body weight) for 6 weeks. Plasma was collected for determination of MDA content (a); femurs were removed for the determination of MDA (b), and t-SH (c). $n=12$ in each group. *CUR* curcumin, *HLS* hind-limb suspension, *MDA* malondialdehyde, *t-SH* total sulfhydryl; * $p<0.05$ versus control group; # $p<0.05$ versus the HLS group

oxidative stress occurred in the femur and lumbar vertebra of rats exposed to modeled microgravity [15], which was confirmed in the current study. In addition, it was found that modeled microgravity exposure induced oxidative stress in

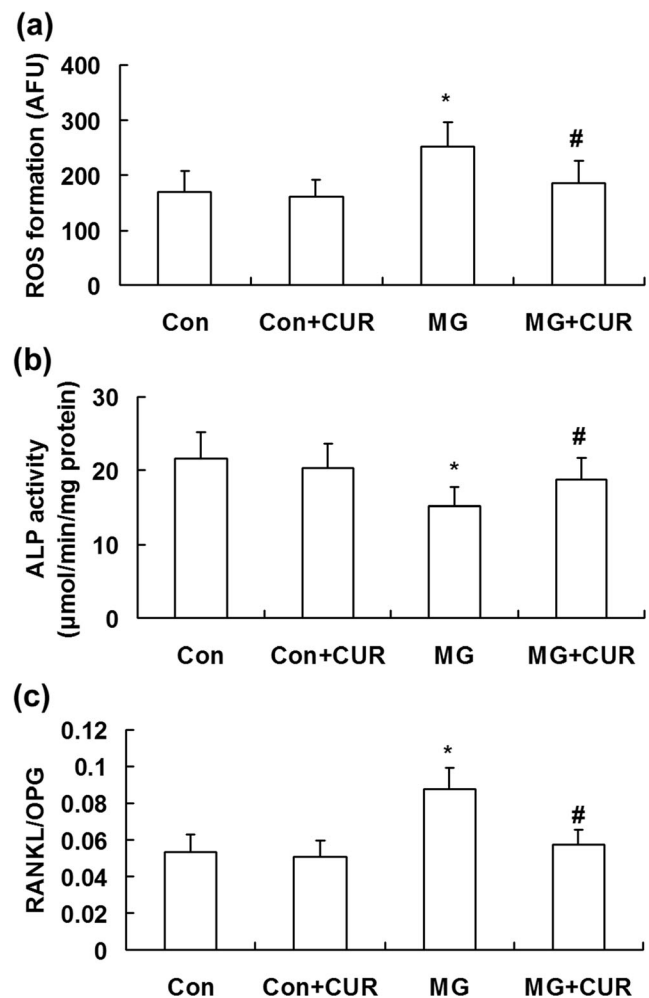


Fig. 4 Treatment with curcumin enhances osteoblast differentiation of MC3T3-E1 cells exposed to modeled microgravity. MC3T3-E1 cells were incubated in rotary wall vessel bioreactor and treated with curcumin (4 µM). The intracellular ROS content (a), ALP activity (b), and ratio of RANKL/OPG (c), were determined. *CUR* curcumin, *OPG* osteoprotegerin, *RANKL* receptor activator of NFκB ligand, *ROS* reactive oxygen species, *ALP* alkaline phosphatase, *MG* modeled microgravity, *AFU* arbitrary fluorescence units; * $p<0.05$ versus control group; # $p<0.05$ versus MG group

cultured osteoblasts and osteoclasts. Oxidative stress, resulting from excessive formation of ROS or dysfunction of antioxidant defense system, represents a major cause of age-associated pathological conditions including aging [16] and postmenopausal bone loss [17]. Sun et al. found that HLS-induced bone loss was attenuated by treatment with hydrogen gas, a novel antioxidant [15], which indicated that oxidative stress also played an important role in the progression of microgravity-induced bone loss. The protective features of curcumin, first and foremost its antioxidant effect, have been shown in experimental studies [18, 19]. In this study, treatment with curcumin alleviated HLS-induced oxidative stress in femurs and incubation with curcumin reduced ROS formation in cultured osteoblasts and osteoclasts exposed to modeled microgravity.

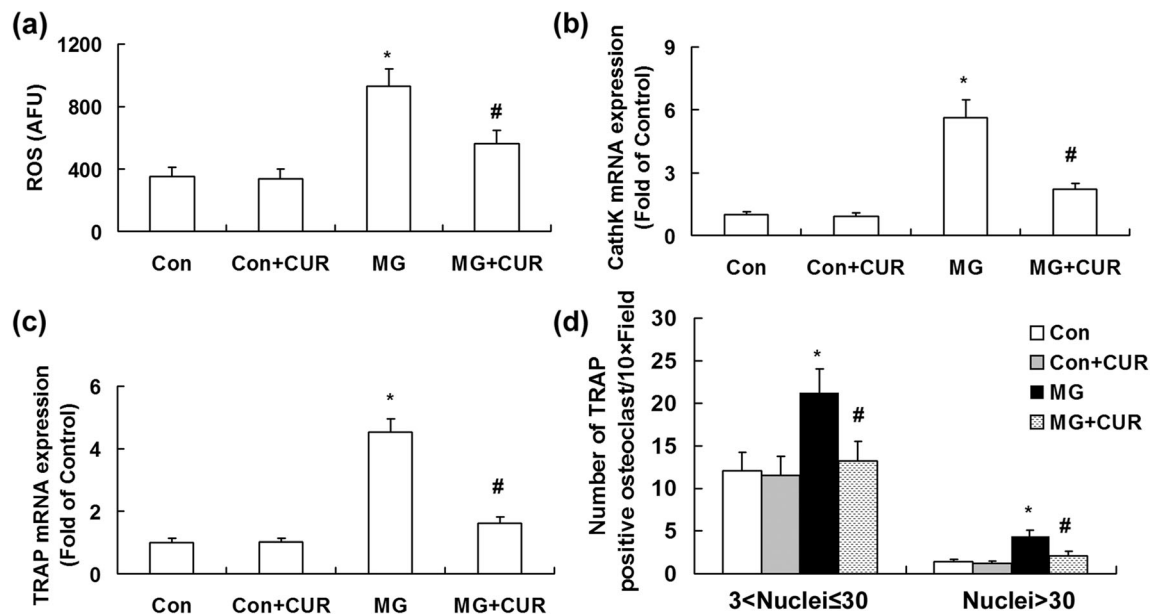


Fig. 5 Treatment with curcumin reduces osteoclast differentiation of RAW264.7 cells exposed to modeled microgravity. RAW264.7 cells were incubated in rotary wall vessel bioreactor and treated with curcumin (4 μ M). Osteoclast differentiation and osteoclastogenesis were induced by incubation with RANKL (20 ng/ml). The intracellular ROS content (a), CathK (b), and TRAP mRNA expression (c), and

multinucleated TRAP-positive cells (d) were determined. CUR curcumin, RANKL receptor activator of NF κ B ligand, MG modeled microgravity, CathK cathepsin K, TRAP tartrate-resistant acid phosphatase, AFU arbitrary fluorescence units; * p <0.05 versus the control group; # p <0.05 versus the MG group

Treatment with curcumin enhanced osteocalcin expression in bone and decreased urinary DPD excretion, indicating that curcumin had beneficial effect on both bone formation and bone resorption when exposed to microgravity. Then, the protective effect of curcumin on osteoblast cell line MC3T3-E1 and preosteoclast cell line RAW264.7 was investigated.

In the current study, microgravity modeled by rotating wall vessel bioreactor suppressed differentiation of MC3T3-E1 cells marked by decreased ALP activity. Some reports have reported that curcumin at high concentration (>10 μ M) markedly inhibited the proliferation of rat calvarial osteoblastic cells and induced the death of human osteoblasts [20–22]. Gu et al. demonstrated that curcumin (10 μ M) promoted rat mesenchymal stem cell osteoblast differentiation by upregulation of HO-1 [23]. In this study, incubation with curcumin increased osteoblastic differentiation of MC3T3-E1 cells exposed to modeled microgravity and had no significant effect on MC3T3-E1 cells under control condition, which might be contributed to the low dose of curcumin we chose in this study.

Curcumin also acts as an inhibitor of RANKL-induced NFATc1 which is a downstream event of NF- κ B signal pathway through suppressing of ROS generation [24], leading to suppressed proliferation, induced chemosensitization, and suppressed osteoclastogenesis [25–27]. Osteoclasts are activated by binding of the RANKL [28] to its cognate receptor, RANK, whereas OPG, a soluble member of the tumor necrosis receptor super-family, acts as a naturally occurring decoy

receptor that competes with RANK for binding of RANKL [29]. The balance of these two molecules plays a critical role in the control of osteoclastogenesis. In the present study, it was found that modeled microgravity increased the ratio of RANKL/OPG. Therefore, modeled microgravity might exacerbate the osteoclastogenesis through paracrine regulation of the release of OPG and RANKL from osteoblasts. Curcumin treatment reduced the formation of ROS and the ratio of RANKL/OPG, which might explain its suppressive effect on osteoclastogenesis induced by modeled microgravity.

Microgravity exposure has been associated with changes in the vitamin D endocrine system. Serum levels of vitamin D hormone were decreased after long-term bed rest [30, 31], and after long-term space flight [32, 33]. The preponderance of evidence indicates that 1,25-(OH) $_2$ D $_3$ enhances bone mineralization through its effects to promote calcium and phosphate absorption [34]. VDR is a nuclear transcription factor, which mediates the action of 1,25-(OH) $_2$ D $_3$, thus affecting calcium absorption, bone remodeling, and mineralization rate [35]. Narayanan et al. first reported that modeled microgravity reduced VDR expression in cultured MG-63 cells [36]. Our results revealed that HLS led to downregulation of VDR expression in femur and modeled microgravity reduced VDR mRNA levels in cultured osteoblasts. As another potential ligand for the VDR, curcumin upregulated VDR expression and activated VDR target genes in osteosarcoma and Caco-2 cells [10]. In this work, although curcumin treatment had no significant effect on serum 1,25-(OH) $_2$ D $_3$ levels, it

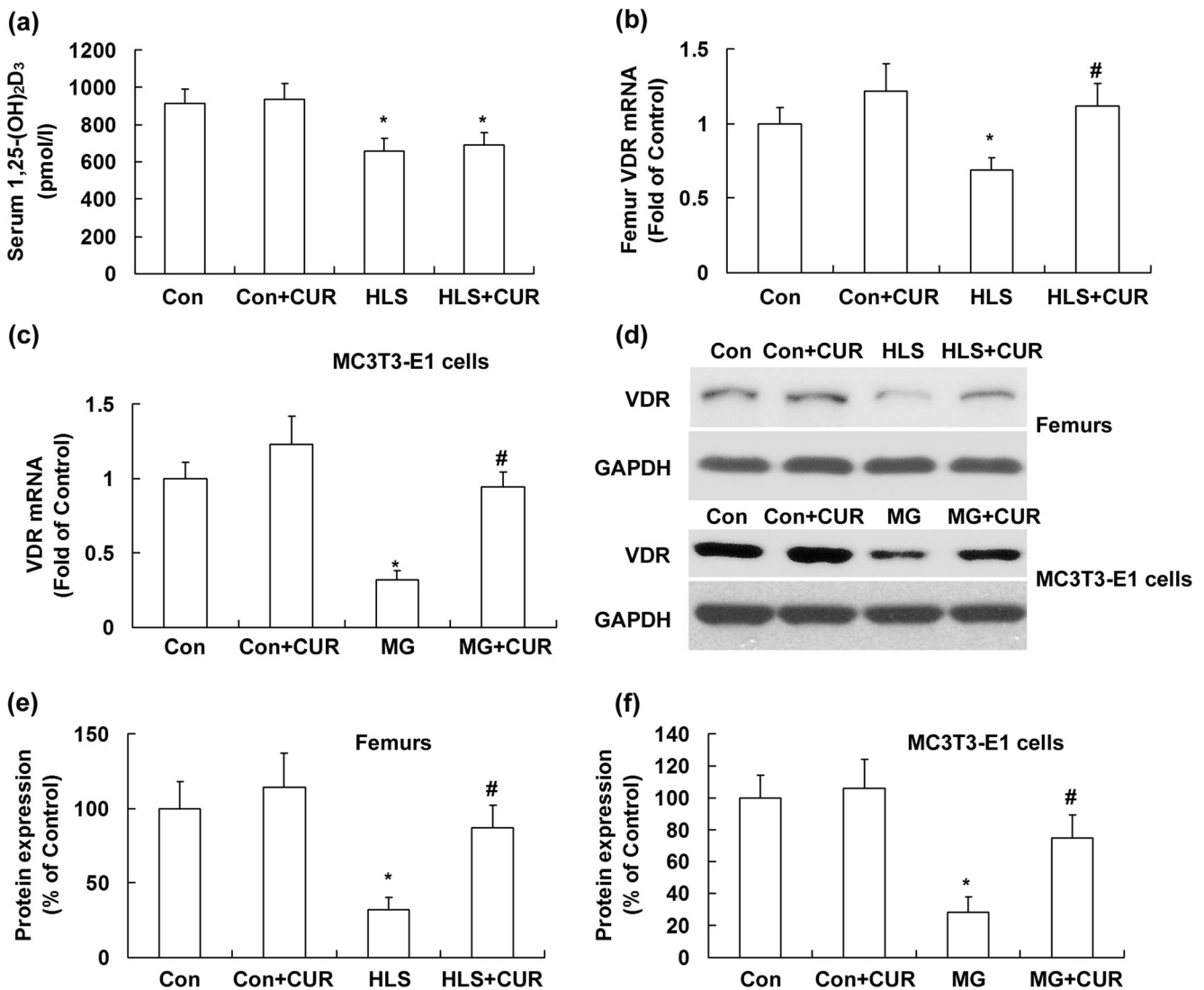


Fig. 6 Treatment with curcumin has no significant effect on serum vitamin D but upregulates VDR expression. SD rats were exposed to HLS and treated with or without curcumin (40 mg/kg body weight) for 6 weeks. Serum was collected for determination of 1,25-(OH)₂D₃ content (a); femurs were removed for the determination of VDR mRNA expression (b). $n=12$ in each group. * $p<0.05$ versus the control group; # $p<0.05$ versus the HLS group. MC3T3-E1 cells were incubated in

RWVB and treated with curcumin (4 μ M). The mRNA levels of VDR (c) were determined. Western blotting results (d) and responding quantification (e, f) of VDR in femurs of rats exposed to HLS or in MC3T3-E1 cells incubated in RWVB were shown. * $p<0.05$ versus the control group; # $p<0.05$ versus the MG group. CUR curcumin, RWVB rotary wall vessel bioreactor, HLS hind-limb suspension, MG modeled microgravity; VDR vitamin D receptor

upregulated VDR expression in femurs and osteoblasts, which might contribute to the beneficial effect of curcumin against bone loss induced by microgravity.

Another important issue of curcumin treatment is its dosage, duration, and mode of administration. Curcumin was found to induce bone changes after ovariectomy in a dose-dependent manner [5]. The dose used was claimed to be safe as there have been no reports of significant adverse effects with the consumption of 500 to 8000 mg turmeric powder/day in humans [37, 38]. The 110-mg/kg dose of curcumin was used in rats orally and no significant side effect was reported [6]. Curcumin treatment (40 mg/kg) for 6 weeks itself had no significant effect on bone geometric and microstructural

parameters of control rats in this work. Long-term studies have shown that curcumin applied in the diet is fully safe and can possess protective activity. Even very high doses of curcumin (8 g/day) did not cause side effects [38]. Even though there is little information about the negative effects of curcumin provided in diet, in vitro curcumin can induce apoptosis of both normal and cancer cells [39]. At high concentration, curcumin induced detrimental effects, including cell senescence, even cell death, which was found in cancer MCF7, HCT116, and U2OS cells [40] and cancer-associated fibroblasts [41]. It is not difficult to imagine that acceleration of senescence of normal cells could be detrimental. It was reported that curcumin induced senescence of primary human

cells building the vasculature in a DNA damage and ataxia-telangiectasia mutated-independent manner [42]. Therefore, further investigation was required and an increase in the bioavailability of curcumin should be introduced very carefully considering senescence induction as a side effect.

In conclusion, treatment with curcumin attenuated microgravity-induced bone loss, possibly through abating oxidative stress and activating vitamin D receptor. Curcumin might be an effective countermeasure for microgravity-induced bone loss but further studies are required to identify this issue before clinical application becomes possible.

Acknowledgments We give our heartfelt thanks to Professor Rachel Lee (The Medical School, The Australian National University) for her support and help throughout the research.

Conflicts of interest None

References

- Blanc S, Normand S, Ritz P, Pachiaudi C, Vico L, Gharib C, Gauquelin-Koch G (1998) Energy and water metabolism, body composition, and hormonal changes induced by 42 days of enforced inactivity and simulated weightlessness. *J Clin Endocrinol Metab* 83:4289–4297
- Kim H, Iwasaki K, Miyake T, Shiozawa T, Nozaki S, Yajima K (2003) Changes in bone turnover markers during 14-day 6 degrees head-down bed rest. *J Bone Miner Metab* 21:311–315
- Zhang DW, Fu M, Gao SH, Liu JL (2013) Curcumin and diabetes: a systematic review. *Evid Based Complement Alternat Med* 2013: 636053
- Zhou H, Beevers CS, Huang S (2011) The targets of curcumin. *Curr Drug Targets* 12:332–347
- French DL, Muir JM, Webber CE (2008) The ovariectomized, mature rat model of postmenopausal osteoporosis: an assessment of the bone sparing effects of curcumin. *Phytomedicine* 15:1069–1078
- Hussan F, Ibraheem NG, Kamarudin TA, Shuid AN, Soelaiman IN, Othman F (2012) Curcumin protects against ovariectomy-induced bone changes in rat model. *Evid Based Complement Alternat Med* 2012:174916
- Zhou T, Chen D, Li Q, Sun X, Song Y, Wang C (2013) Curcumin inhibits inflammatory response and bone loss during experimental periodontitis in rats. *Acta Odontol Scand* 71:349–356
- Yang MW, Wang TH, Yan PP, Chu LW, Yu J, Gao ZD, Li YZ, Guo BL (2011) Curcumin improves bone microarchitecture and enhances mineral density in APP/PS1 transgenic mice. *Phytomedicine* 18:205–213
- Dinkova-Kostova AT, Talalay P (2008) Direct and indirect antioxidant properties of inducers of cytoprotective proteins. *Mol Nutr Food Res* 52:S128–S138
- Bartik L, Whitfield GK, Kaczmarek M, Lowmiller CL, Moffet EW, Furnick JK, Hernandez Z, Haussler CA, Haussler MR, Jurutka PW (2010) Curcumin: a novel nutritionally derived ligand of the vitamin D receptor with implications for colon cancer chemoprevention. *J Nutr Biochem* 21:1153–1161
- Zayzafoon M, Gathings WE, McDonald JM (2004) Modeled microgravity inhibits osteogenic differentiation of human mesenchymal stem cells and increases adipogenesis. *Endocrinology* 145: 2421–2432
- Bouxsein ML, Boyd SK, Christiansen BA, Guldberg RE, Jepsen KJ, Müller R (2010) Guidelines for assessment of bone microstructure in rodents using micro-computed tomography. *J Bone Miner Res* 25:1468–1486
- Saxena R, Pan G, Dohm ED, McDonald JM (2011) Modeled microgravity and hindlimb unloading sensitize osteoclast precursors to RANKL mediated osteoclastogenesis. *J Bone Miner Metab* 29: 111–122
- Rai B, Kaur J, Catalina M, Anand SC, Jacobs R, Teughels W (2011) Effect of simulated microgravity on salivary and serum oxidants, antioxidants, and periodontal status. *J Periodontol* 82:1478–1482
- Sun Y, Shuang F, Chen DM, Zhou RB (2013) Treatment of hydrogen molecule abates oxidative stress and alleviates bone loss induced by modeled microgravity in rats. *Osteoporos Int* 24:969–978
- Linnane AW, Eastwood H (2006) Cellular redox regulation and prooxidant signaling systems, a new perspective on the free radical theory of aging. *Ann N Y Acad Sci* 1067:7
- Sendur OF, Turan Y, Tastaban E, Serter M (2009) Antioxidant status in patients with osteoporosis, a controlled study. *Joint Bone Spine* 76:514
- Hemeida RA, Mohafez OM (2008) Curcumin attenuates methotrexate-induced hepatic oxidative damage in rats. *J Egypt Natl Cancer Inst* 20:141–148
- Fleenor BS, Sindler AL, Marvi NK, Howell KL, Zigler ML, Yoshizawa M, Seals DR (2013) Curcumin ameliorates arterial dysfunction and oxidative stress with aging. *Exp Gerontol* 48:269–276
- Moran JM, Roncero-Martin R, Rodriguez-Velasco FJ, Calderon-Garcia JF, Rey-Sanchez P, Vera V, Canal-Macias ML, Pedrera-Zamorano JD (2012) Effects of curcumin on the proliferation and mineralization of human osteoblast-like cells: implications of nitric oxide. *Int J Mol Sci* 13:16104–16118
- Notoya M, Nishimura H, Woo JT, Nagai K, Ishihara Y, Hagiwara H (2006) Curcumin inhibits the proliferation and mineralization of cultured osteoblasts. *Eur J Pharmacol* 534:55–62
- Chan WH, Wu HY, Chang WH (2006) Dosage effects of curcumin on cell death types in a human osteoblast cell line. *Food Chem Toxicol* 44:1362–1371
- Gu Q, Cai Y, Huang C, Shi Q, Yang H (2012) Curcumin increases rat mesenchymal stem cell osteoblast differentiation but inhibits adipocyte differentiation. *Pharmacogn Mag* 8:202–208
- Moon HJ, Ko WK, Han SW, Kim DS, Hwang YS, Park HK, Kwon IK (2012) Antioxidants, like coenzyme Q10, selenite, and curcumin, inhibited osteoclast differentiation by suppressing reactive oxygen species generation. *Biochem Biophys Res Commun* 418:247–253
- Kim JH, Gupta SC, Park B, Yadav VR, Aggarwal BB (2012) Turmeric (*Curcuma longa*) inhibits inflammatory nuclear factor (NF)- κ B and NF- κ B-regulated gene products and induces death receptors leading to suppressed proliferation, induced chemosensitization, and suppressed osteoclastogenesis. *Mol Nutr Food Res* 56:454–465
- Park SK, Oh S, Shin HK, Kim SH, Ham J, Song JS, Lee S (2011) Synthesis of substituted triazolyl curcumin mimics that inhibit RANKL-induced osteoclastogenesis. *Bioorg Med Chem Lett* 21: 3573–3577
- Oh S, Kyung TW, Choi HS (2008) Curcumin inhibits osteoclastogenesis by decreasing receptor activator of nuclear factor- κ B ligand (RANKL) in bone marrow stromal cells. *Mol Cells* 26:486–489
- Kong YY, Yoshida H, Sarosi I, Tan HL, Timms E, Capparelli C, Morony S, Oliveira-dos-Santos AJ, Van G, Itie A, Khoo W, Wakeham A, Dunstan CR, Lacey DL, Mak TW, Boyle WJ, Penninger JM (1999) OPGL is a key regulator of osteoclastogenesis, lymphocyte development and lymph-node organogenesis. *Nature* 397:315–323

29. Suda T, Takahashi N, Udagawa N, Jimi E, Gillespie MT, Martin TJ (1999) Modulation of osteoclast differentiation and function by the new members of the tumor necrosis factor receptor and ligand families. *Endocr Rev* 20:345–357
30. Zerwekh JE, Odvina CV, Wuermsler L-A, Pak CYC (2007) Reduction of renal stone risk by potassiummagnesium citrate during 5 weeks of bed rest. *J Urol* 177:2179–2184
31. Zerwekh JE, Ruml LA, Gottschalk F, Pak CYC (1998) The effects of twelve weeks of bed rest on bone histology, biochemical markers of bone turnover, and calcium homeostasis in eleven normal subjects. *J Bone Miner Res* 13:1594–1601
32. Smith SM, Wastney ME, Morukov BV, Larina IM, Nyquist LE, Abrams SA, Taran EN, Shih CY, Nillen JL, Davis-Street JE, Rice BL, Lane HW (1999) Calcium metabolism before, during, and after a 3-mo spaceflight: kinetic and biochemical changes. *Am J Physiol* 277:R1–R10
33. Zittermann A, Heer M, Caillot-Augusso P, Rettberg P, Scheld K, Drummer C, Alexandre C, Horneck G, Vorobiev D, Stehle P (2000) Microgravity inhibits intestinal calcium absorption as shown by a stable strontium test. *Eur J Clin Investig* 30:1036–1043
34. Yoshida T, Stern PH (2012) How vitamin D works on bone. *Endocrinol Metab Clin N Am* 41:557–569
35. Pike JW, Yamamoto H, Shevde NK (2002) Vitamin D receptormediated gene regulation mechanisms and current concepts of vitamin D analog selectivity. *Adv Ren Replace Ther* 9: 168–174
36. Narayanan R, Smith CL, Weigel NL (2002) Vector-averaged gravity-induced changes in cell signaling and vitamin D receptor activity in MG-63 cells are reversed by a 1,25-(OH)2D3 analog, EB1089. *Bone* 31:381–388
37. Chandran B, Goel A (2012) A randomized, pilot study to assess the efficacy and safety of curcumin in patients with active rheumatoid arthritis. *Phytother Res* 26:1719–1725
38. Cheng AL, Hsu CH, Lin JK, Hsu MM, Ho YF, Shen TS, Ko JY, Lin JT, Lin BR, Ming-Shiang W, Yu HS, Jee SH, Chen GS, Chen TM, Chen CA, Lai MK, Pu YS, Pan MH, Wang YJ, Tsai CC, Hsieh CY (2001) Phase I clinical trial of curcumin, a chemopreventive agent, in patients with high-risk or pre-malignant lesions. *Anticancer Res* 21:2895–2900
39. Bielak-Zmijewska A, Koronkiewicz M, Skierski J, Piwocka K, Radziszewska E, Sikora E (2000) Effect of curcumin on the apoptosis of rodent and human nonproliferating and proliferating lymphoid cells. *Nutr Cancer* 38:131–138
40. Mosieniak G, Adamowicz M, Alster O, Jaskowiak H, Szczepankiewicz AA, Wilczynski GM, Ciecchomska IA, Sikora E (2012) Curcumin induces permanent growth arrest of human colon cancer cells: link between senescence and autophagy. *Mech Ageing Dev* 133:444–455
41. Hendrayani SF, Al-Khalaf HH, Aboussekhra A (2013) Curcumin triggers p16-dependent senescence in active breast cancer-associated fibroblasts and suppresses their paracrine procarcinogenic effects. *Neoplasia* 15:631–640
42. Grabowska W, Kucharewicz K, Wnuk M, Lewinska A, Suszek M, Przybylska D, Mosieniak G, Sikora E, Bielak-Zmijewska A (2015) Curcumin induces senescence of primary human cells building the vasculature in a DNA damage and ATM-independent manner. *Age (Dordr)* 37:9744